Proceeding of the 13th National Mechanical Engineering Conference
2-3 December 1999, Royal Cliff Beach Resort Hotel, South Pattaya, Cholburi

On The Decay of Characteristic Mean Temperature of A Heated Swirling Jet

Weerin Wangjiraniran, Pongput Uppathamnarakorn and Asi Bunyajitradulya

Fluid Mechanics Research Laboratory, Department of Mechanical Engineering,
Faculty of Engineering, Chulalongkorn University,
Bangkok 10330, Thailand
Tel. 218-6645, 218-6647; Fax. 252-2889; E-mail basi@chula.ac.th

Abstract

Experiments for the investigation of the effect of swirl number on the mixing characteristics of a swirling jet were conducted. The configuration chosen was that of a heated swirling jet and the indicator for mixing efficiency was the decay of the characteristic mean temperature. The heated swirling jet was generated by passing hot air through a rotating pipe with honeycomb. The experiments were performed at Reynolds number of approximately 4,000 and the swirl number was varied from 0 (no swirl), 0.3, 0.6, to 0.9. The initial condition chosen, in contrast to past works, was that of the approximate of pipe flow. The results indicated linear reduction in $x_{50\%}$, from 7.5 for non-swirling jet to 4 for swirling jet with the swirl number of 0.9, with increase in swirl number. In addition, increase in the decay rate and decrease in the extent of the potential core were observed. This showed that swirling jets stir more efficiently than non-swirling jets, and that as the swirl number increases, the stirring efficiency increases. Finally, the linear reduction in $x_{50\%}$ at the end of the range of swirl numbers investigated, i.e., 0.9, suggested that further increase in stirring efficiency may still be possible at higher swirl number.

1.Introduction

Swirling jet is a flow of many technological applications. It is used to enhance mixing in a combustion chamber, to increase the ratio of heat transfer to the required pumping power, to develop active shear-layer control, etc. Characteristics of swirling jets are neatly summarized by Feyedelem and Sarpkaya (1997). We briefly state some of them here.

In comparison to a non-swirling jet, a jet with swirl entrains more rapidly, and thus spreads more rapidly and displays a more rapid decay of mean velocity. As a result, the initial expansion of the jet is followed by a steady decrease in the spreading rate, and after about 10 diameters the influence of swirl becomes negligible and the jet characteristics asymptotes to a non-swirling state.

The flow characteristics in the near filed of a swirling jet are significantly influenced by the initial tangential velocity distribution. Therefore, it was suggested that the swirl number, S, may not be adequate in describing the characteristics of the jet.

Owing to streamline curvature generated by the swirl, static pressure gradients exist across the flow. Consequently the spreading rate in the near field of the jet is mainly influenced by pressure rather than by turbulent mixing as in the case of a non-swirling jet.

For strongly swirling jets, the maximum axial velocity may be displaced from the jet axis, and recirculation zone may form in the nozzle or near the jet exit. If suitable conditions are present, vortex breakdown may occur and will have profound effects on the jet; the axial velocity distribution changes and reverse flow may be present. Nonetheless, it was found that at $S = 0.48$ to 0.50 the breakdown may occur without reverse flow.

Billant et al. (1998) studied the various breakdown states for a swirling water jet as a function of the swirl number and the Reynolds number, *Re*. The swirl number was varied between 0-1.42 and the Reynolds number between 300-1200. It was found that breakdown occurred when the swirl number reached a well-defined threshold of 1.3-1.4, which was independent of *Re*. Four types of breakdown were identified: bubble, cone, and two associated asymmetric bubble and asymmetric cone. The last two occurred only at high *Re*.

A remark needs to be made regarding the definition of the swirl number. Many authors use many different definitions: some based on the corresponding velocity components, some on the corresponding angular momentum flux components. This depends in part on the flow configuration (e.g., swirling jet, swirling pipe, leading/trailing edge vortices, etc.) as well as the type of initial condition investigated (initial axial and tangential velocity profiles). Thus, in comparing quantitative results, one needs to take this into consideration.

Other studies of swirling jets are by, for example, Farokhi et al. (1988), Wu et al. (1992), Panda and Mclaughlin (1994), and Naughton et al. (1997). And there are considerable amounts of past work on the

related topic of vortex breakdown. We give some examples here as those by Hall (1972), Leibovich (1978), and Escudier and Zehnder (1982)

The present study focuses on the effect of swirl number on the mixing characteristics at large-scale level, the mechanism of which is often called *stirring*, of a swirling jet. The chosen indicator of mixing rate in this case is the decay of the characteristic mean temperature along the streamwise direction, thus a heated swirling jet is employed. The swirling motion is generated by a rotating pipe with a honeycomb. In contrast to past works, the initial axial velocity profile in this study is approximate that of a pipe flow. For this study, the swirl numbers are 0 (no swirl), 0.3, 0.6, and 0.9, and the Reynolds number is 4000.

2. Mixing at large-scale and decay of characteristic mean temperature

In comparison with laminar flows, mixing in turbulent flows is more efficient owing to *stirring*. Briefly, stirring is a mechanism by which large-scale motion entrains surrounding fluid from different parts and "mix" them together. In effect, mixing at large-scale causes effective increase in contact surface initially, thus helps promoting further mixing at small- and, eventually, molecular-scale. Owing to the lack of this process in laminar flows, mixing in laminar flows is much less efficient. It is to be noted, however, that chemical reaction such as combustion process requires mixing at molecular scale.

One of the indicators that are generally used as indicative of mixing efficiency, at least approximately and at large-scale, is the decay of mean quantity such as velocity, temperature, etc, in the streamwise direction. The reason is that, for example, for a heated jet if mixing is efficient, one expects the jet to entrain surrounding cold fluid into the jet and mix it with the hot jet fluid rapidly, resulting in a fast decay of jet temperature as it evolves downstream, and vice versa. Generally, the centerline temperature is used for this purpose because the temperature is maximum there and, equally or more importantly, the intermittency factor (see, for example, Tennekes and Lumley, 1972) is generally maximum at this location.

For this study, however, we avoid the use of exact centerline temperature owing to the fact that, as Feyedelem and Sarpkaya summarized, for strongly swirling jets, the maximum is likely to be displaced from the jet axis. Instead, we employ the maximum mean temperature along one of the traverse passing through the geometric centerline of the pipe (see more details in Sec. 3) as the characteristic mean temperature. The results are then presented in terms of the temperature coefficient C_T at this maximum. The temperature coefficient C_T is defined as

$$C_T = \frac{T - T_R}{T_J - T_R}, \qquad (1)$$

where T is temperature at the measurement location, T_R is surrounding temperature, and T_J is the temperature at the center of the jet exit.

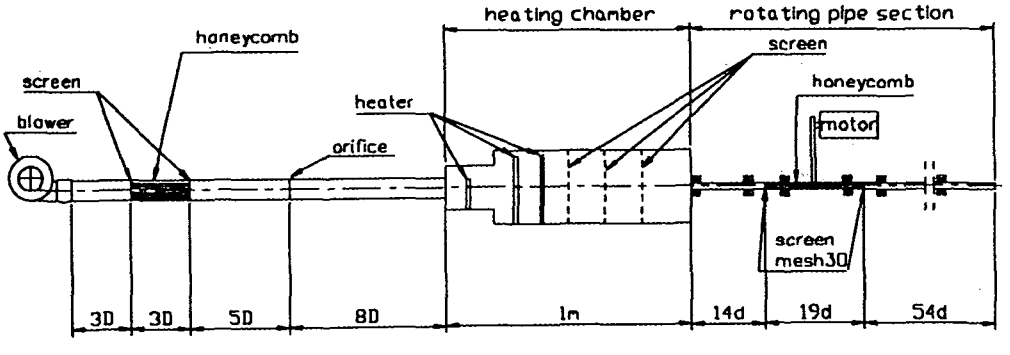

Fig. 1. The swirling jet facility. (D = 75 mm, d = 21 mm)

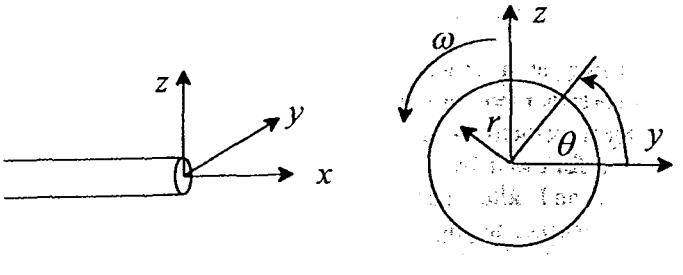

Fig. 2. Coordinates system.

3. Experimental setup

The experiments were conducted in the Fluid Mechanics Research Laboratory (FMRL), Department of Mechanical Engineering, Faculty of Engineering, Chulalongkorn University. The swirling jet facility is shown in Fig. 1, and Fig. 2 shows the coordinates system employed. The setup comprises mainly of three sections: the upstream PVC pipe, the heating chamber, and the downstream rotating pipe. The upstream PVC pipe section is used for monitoring the flowrate via an orifice. The main components in this section are a blower, a flexible duct, a drinking-straw honeycomb sandwiched between two mesh-16 screens (household screens), and an orifice. The pipe used in this section is a 3-inch PVC pipe (ID=75 mm). The blower is used for supplying air through the test rig, the flexible duct for isolating vibration from the blower to the rest of the rig, the honeycomb for conditioning the flow before it enters the orifice, and the orifice for monitoring the flowrate.

The heating chamber heats air to a desired temperature. The main components in this section are two 2000-watt and one 500-watt heaters, a 10 kVA variac, and three screens of open area ratio of 0.5. The variac is used for adjusting the voltage applied to the heaters, thus the heat rate. The screens are employed downstream of the heaters to stir, thus, to make the air temperature distribution more uniform before it enters the rotating pipe section.

The rotating pipe section is made from sections of stainless steel pipes of inner diameter, d, of 21.4 mm and outer diameter of 25 mm. This section is divided into three subsections joined together by two collars. The first subsection, next to the heating chamber, is an idler of $14d$ long. The second subsection, a honeycomb, is of $19d$ long and is filled with sections of brass tube with ID of 3.5 mm, OD of 4.5 mm, and nominally equal length to that of the outer stainless steel pipe, i.e., $19d$. A few smaller tubes are also used to fill the gaps at the edge. The honeycomb is sandwiched between two screens of mesh-30. The third subsection, a developing section, is an idler of $54d$ long. It is used as a straight section to allow the flow to settle before leaving the exit.

To avoid the effect of the ground, the centerline of the rig is placed at 140 cm, or $65d$, above the floor. Generally, clear space of at least $35d$ is provided all around and all along the jet axis, of at least $46d$ in the downstream direction and without any wall-like obstacle placed normally and directly beyond that for another 4 m, and of at least $10d$ upstream of the exit plane of the jet. Due to high rotational speed and the cantilever-like of the jet exit, further extension beyond $10d$ from the support can be done with some cautions.

The rotating pipe section is driven by a 2-hp, 2830 RPM motor and a variable speed inverter. Swirl number is then varied by changing the rotational speed of the motor. The rotational speed of the rotating pipe is then measured by a tachometer.

Flow diagnostics include measurements of initial profiles and of the distribution of characteristic mean temperature. The measurements of the initial "velocity" profiles for both axial (x) and tangential (θ) components are done by means of a pitot probe (ID=0.8 mm, OD=1.2 mm) described in the companion paper by Sakulyanontvittaya et al. (1999). Owing to static pressure gradient within the flow, the reading from pitot probe is not a true reflection of local velocity. Therefore, we present the results in terms of the coefficient of pitot pressure C_P, defined as

$$C_P = \frac{p - p_C}{p_E - p_C}, \qquad (2)$$

where p is local pitot pressure, p_C is pitot pressure at the center of the pipe exit, and p_E is the average pitot pressure over two points at both ends of the traverse. When each component is measured, the probe is aligned such that it is parallel to that component. We shall designate C_P in the axial direction as C_{Px} and in the tangential direction as $C_{P\theta}$.

The measurements of initial temperature profile and the characteristic mean temperature are done by means of a thermocouple. In finding the characteristic mean temperature at any cross section, the thermocouple is traversed at 2 mm step along the z-axis passing through the geometric centerline of the jet, and the maximum temperature along this axis is taken as the characteristic mean temperature for Eq. 1.

The spatial resolutions for measurements are generally 2 mm for initial profiles and $\frac{1}{2}d$ to $1d$ for characteristic mean temperature decay.

For this study we define the swirl number as the ratio between the angular velocity of the pipe ($\omega d/2$) and the mean axial velocity of the jet at the jet exit. Four values of swirl number are tested: 0 (no swirl), 0.3, 0.6, and 0.9. We shall designate these cases as S0, S0.3, S0.6, and S0.9, respectively. The direction of rotation is such that the swirl vector is in the $+x$ direction. The Reynolds number is fixed at 4,000. The mean axial velocity is approximated from pitot readings.

Finally, in all cases the jet is heated to approximately 64-66 °C (slightly change from case to case, but stay practically constant in any one case), and the room temperature during the experiment stays within 32-33 °C. The thermocouple reading is accurate within $\pm$ 1°C.

4. Results and discussion

Initial Conditions

Figures 3 to 5 show the initial profiles for C_{px} (along y- and z-axes), $C_{p\theta}$ (along y-axis), and C_T (along y- and z-axes), respectively. In all these cases, we take the edges as the position $r = \pm$ 10mm. C_{px}'s are quite symmetric and similar for all cases. On the other hand, $C_{p\theta}$'s are less symmetric, especially as S increases and towards the edges, and there are some deviations between

cases. Nonetheless, they are fairly similar. In the figure we also give the estimate curve-fit for case S0.3 together with the goodness of fit. C_T's are generally symmetric and similar although some deviations between cases are observed along the edges. From these results, it is seen that the initial profiles for all cases are fairly similar and swirling flows are fairly well established.

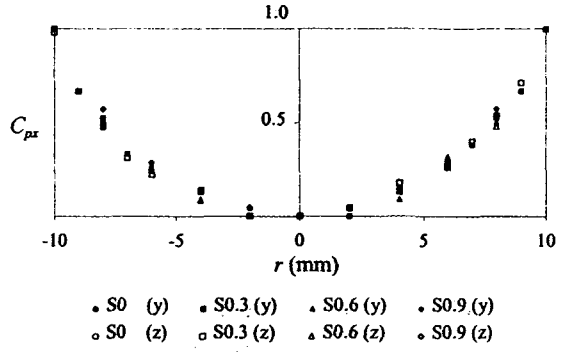

Fig. 3. Initial profiles in the axial direction.

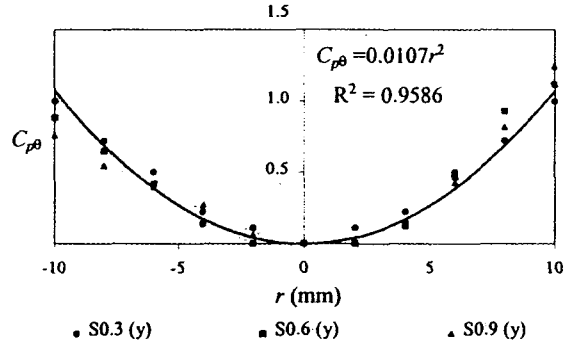

Fig. 4. Initial profiles in the tangential direction.

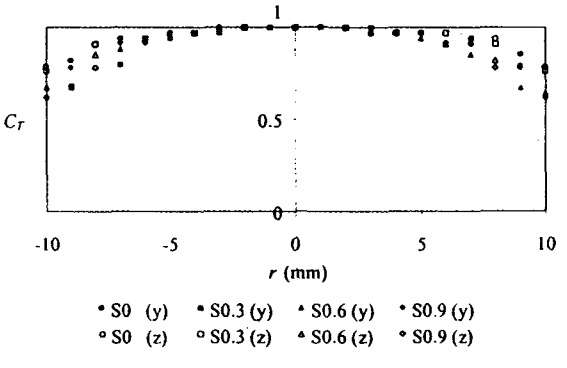

Fig. 5. Initial temperature profiles.

Characteristic mean temperature decay

Figure 6 shows the results for the characteristic mean temperature distribution. As the swirl number increases, the rate of temperature drop increases, especially within the first 5-6 diameters. We give the estimate of the downstream distance for which C_T reduces to half, $x_{50\%}$, as follows: S0, 7.5*d*; S0.3, 6*d*; S0.6, 5*d*; and S0.9, 4*d*. A glance at these figures suggests that $x_{50\%}$ is inversely and linearly proportional to the swirl number. Figure 7 shows the same plot on the semi-log. As one can see, the decay rate increases as the swirl number increases.

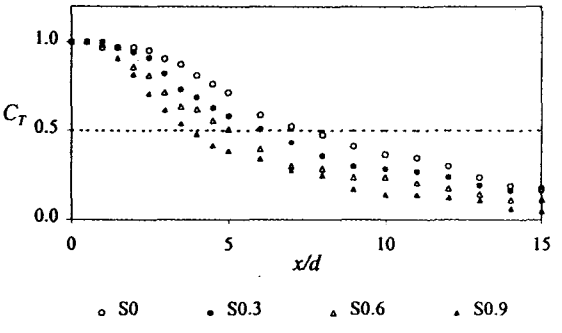

Fig. 6. Characteristic mean temperature distributions.

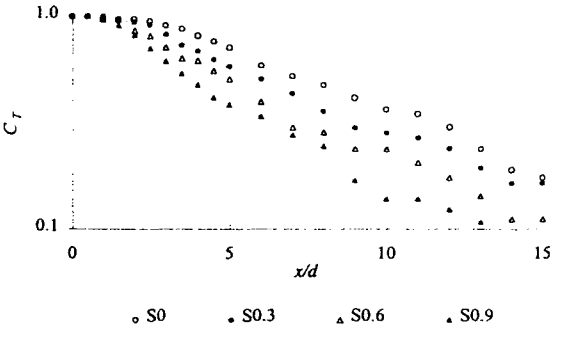

Fig. 7. A replot of Fig.6 on a semi-log showing the decay rates.

In addition, Fig. 6 indicates that the extent of the "potential" core decreases with increase in the swirl number.

The reduction in $x_{50\%}$, the increase in the decay rate, and the reduction in the extent of the potential core, with increase in swirl number suggest that swirling jets stir more efficiently than non-swirling jets, and that as the swirl number increases, the stirring efficiency increases. More importantly, owing to the linear relation between $x_{50\%}$ and the swirl number S in the range of this experiment, i.e., S = 0-0.9, this suggests that further increase in stirring efficiency may still be possible with higher swirl number although, at one point, some limit or reduction in increase in efficiency is expected ($x_{50\%}$ of S0.9 ~ 4d.) This shall be part of our further investigation on swirling jets.

5. Conclusions

The effect of swirl number on the stirring efficiency of a swirling jet was investigated. A heated swirling jet was chosen as the test configuration and the decay of the

characteristic mean temperature was chosen as an indicator. The experiments were performed at the Reynolds number of approximately 4,000 and the swirl number was varied from 0, 0.3, 0.6, to 0.9. The initial condition chosen, in contrast to past works, was that of the approximate of pipe flow.

The results indicated increase in stirring efficiency with increase in swirl number. Specifically, linear reduction in $x_{50\%}$, from 7.5 for non-swirling jet to 4 for swirling jet with swirl number of 0.9, was observed with increase in swirl number. In addition, increase in the decay rate and decrease in the extent of the potential core were observed.

Finally, the linear reduction in $x_{50\%}$ at the end of the range of swirl numbers varied in this study, i.e., 0.9, suggested that further increase in stirring efficiency may still be possible at higher swirl number, an issue for which we shall investigate further as part of our research program on swirling jets.

Acknowledgements

The authors would like to thank Mr. Kiattisak Kobkanjanakorn and Mr. Tosapole Stitsuwongkul, current FMRL graduate students, for their assistance in the construction of the test rig. They also appreciate many helps from, also current FMRL graduate students, Mr.'s Sumeth Tripopsakul, Suthichock Nunthasookkasame, and Parama Phromsuthirak.

References

1. Billant, P., Chomaz, J.-M., and Huerre, P., (1998), "Experimental study of vortex breakdown in swirling jets," *J. Fluid Mech.*, Vol. 376, pp. 183-219.
2. Escudier, M. P., and Zehnder, N., (1982), "Vortex-flow regimes," *J. Fluid Mech.*, Vol. 115, pp. 105-121.
3. Farokhi, S., Taghavi, R., and Rice, E. J., (1988), "Effect of initial swirl distribution on the evolution of a turbulent jet," *AIAA J.*, Vol. 27, pp. 700-706.
4. Feyedelem, M. S., and Sarpkaya, T., (1997), "Free and near-free-surface swirling turbulent jets," AIAA Paper No. 97-0438.
5. Hall, M. G., (1972), "Vortex breakdown," *Ann. Rev. Fluid Mech.*, Vol. 4, pp. 195-218.
6. Leibovich, S., (1978), "The structure of vortex breakdown," *Ann. Rev. Fluid Mech.*, Vol. 10, pp. 221-246.
7. Naughton, J. W., Cattafesta, L. N., and Settles, G. S., (1997), "An experimental study of compressible turbulent mixing enhancement in swirling jets," *J. Fluid Mech.*, Vol. 330, pp. 271-305.
8. Panda, J., and McLaughlin, D. K., (1994), "Experiments on the instabilities of a swirling jet," *Phys. Fluids*, Vol. 6., pp. 263-276.
9. Sakulyanontvittaya, T., Ngow, P., Prasartkarnkha, A., Chalokepunrat, S., Pimpin, A., and Bunyajitradulya, A., (1999), "The Design and Development of The FMRL 60x18 cm^2 Wide-Angle Screened-Diffuser Blower Tunnel Part III: The Settling Chamber, The Contraction, and The Wind Tunnel," Proceeding of the 13th National Mechanical Engineering Conference, 2-3 December 1999, Royal Cliff Beach Resort Hotel, South Pattaya, Cholburi.
10. Tennekes, H., and Lumley, J. L., (1972), A first course in turbulence, The MIT Press, Cambridge.
11. Wu, M. M., Garcia, A., Chomaz, J. M., and Huerre, P., (1992), "Instabilities in a swirling water jet," *Bull. Am. Phys. Soc.*, Vol. 37, p. 1789.